Journal of Materials Chemistry C

PAPER

View Article Online
View Journal | View Issue

Cite this: J. Mater. Chem. C, 2016, 4, 9608

Repeated shape recovery of clustered nanopillars by mechanical pulling†

Sang Moon Kim,‡[ab] Seong Min Kang,‡[bc] Chanseok Lee,[c] Segeun Jang,[c] Junsoo Kim,[d] Hyein Seo,[e] Won-Gyu Bae,[f] Shu Yang*[g] and Hyunsik Yoon*[e]

Received 27th June 2016,
Accepted 12th September 2016

DOI: 10.1039/c6tc02660e

www.rsc.org/MaterialsC

High-aspect-ratio (HAR) nanopillars are of interest for wetting, adhesion, and energy harvesting due to their superior surface properties, including large surface area and high compliance. However, their intrinsically low mechanical stability has been a major obstacle for practical applications that require repeated use and in wet and humid environments. Herein, we show a method that can recover the clustered or deformed HAR nanopillars to their original shapes by taking advantage of the mechanical compliance of the nanopillars toward pulling during a demolding process. The pillars can be repeatedly clustered and recovered many times. Our method is simple yet powerful to recover the clustered nanopillars over a large area (7 × 10 cm^2). By taking advantage of the different optical properties of the clustered pillars *vs.* the straight ones, we demonstrate display and erasing of patterns and tunable wettability by stamping the nanopillars to induce clustering, followed by shape recovery *via* demolding of the pillars.

Introduction

High-aspect-ratio (HAR) nano- and micropillars are of great interest for a wide range of potential applications due to their superior surface properties, including large surface area and high compliance. Inspired by a gecko's foot hair, HAR pillars have been extensively studied as gecko-like dry adhesives.[1,2] The pillar arrays could also be made superhydrophobic because of the ability to trap air pockets between the pillar arrays.[3,4] When HAR pillars with large spacing are decorated with nanoparticles on top, they can be both transparent and amphiphobic (*i.e.*, repelling both water and oil).[5] Nanopillar arrays have also been demonstrated to trap incident light, thus enhancing efficiency in energy harvesting[6] and surface enhanced Raman scattering (SERS),[7] and to manipulate stem cell differentiation for bone generation.[8] However, they can also be easily deformed in a wet or humid environment, where many applications are performed, due to swelling, thus, lowering their modulus, and/or capillary force upon drying[9–11] or simply under a mechanical load above the buckling threshold. When the capillary force and/or the adhesion force between the pillars are greater than the restoring elastic force, neighboring pillars will cluster together. As a result, the ordered straight pillars will lose their properties such as structural color, or transparency.

Approaches to prevent clustering have been developed by using high modulus materials or reinforcing the pillars through partial coating of a thin layer of metal.[12–14] Nevertheless, once the pillars are clustered, it is difficult to recover them.[15–18] It has been demonstrated that tilted micropillar arrays (diameter of 10 μm or larger and aspect ratio, AR = height/diameter, typically no more than 4) made of tilted shape memory polymers can be recovered upon reheating.[19,20] Ultrasonic force has also been demonstrated to recover micropillars with sparse spacing.[21] However, it is not possible to recover heavily clustered, high-density nanopillars with ARs greater than 4. Herein, we demonstrate a facile method to recover the clustered HAR nanopillars (400 nm in diameter and AR = 10) to their original, straight shape during demolding of photocured polymers infiltrated between the nanopillars. The shape recovery process is repeated more than five times. While the straight nanopillar array is highly ordered with reflective colors, the clustered pillars are random and appear opaque. By taking advantage of the difference in the optical properties in the recovered region *vs.* the clustered region, we demonstrate display of letters using a stamp, which can be erased by the demolding process.

[a] Department of Mechanical Engineering, Incheon National University, Incheon, 406-772, Korea
[b] Global Frontier Center for Multiscale Energy System, Seoul National University, Seoul, 151-744, Korea
[c] Department of Mechanical and Aerospace Engineering, Seoul National University, Seoul, 151-742, Korea
[d] Energy Harvesting Devices Research Section, Electronics and Telecommunications Research Institute, Daejeon, 305-700, Republic of Korea
[e] Department of Chemical and Biomolecular Engineering, Seoul National University of Science & Technology, Seoul, 139-743, Korea. E-mail: hsyoon@seoultech.ac.kr
[f] Department of Electrical Engineering, Soongsil University, Seoul, 156-743, Korea
[g] Department of Materials Science and Engineering, University of Pennsylvania, Philadelphia, PA 19104-6272, USA. E-mail: shuyang@seas.upenn.edu

† Electronic supplementary information (ESI) available: The optical image of the Si master and additional SEM images. See DOI: 10.1039/c6tc02660e

‡ S. M. Kim and S. M. Kang contributed equally to this work.

Experimental

Fabrication of the Si master

A thin SiO_2 layer (500 nm thickness) was developed on a pre-cleaned silicon wafer by a thermal oxidation process. A square array of a hole pattern (400 nm in diameter) was fabricated on the SiO_2 layer by the conventional photolithography and oxide etching process. After that, the wafer was etched by SF_6 gas plasma in an inductively coupled plasma (ICP) chamber to make HAR holes. Finally, octafluorocyclobutane (C_4F_8) was deposited on the Si master by ICP plasma treatment at 30 mTorr for 20 s to form a thin and conformal hydrophobic coating (50 nm) to lower the surface energy of the Si master.[22]

Preparation of polymeric HAR nanopillars

The UV-curable precursors, soft polyurethane acrylate (PUA, MINS 301, Minuta Tec.), hard PUA (MINS 311, Minuta Tec.) and NOA 71 (Sigma Aldrich, Korea), were dispensed on the above fabricated Si master and a 50 μm-thick poly(ethylene terephthalate) (PET) film was gently placed on top of the precursor droplets as the substrate. After UV-curing (λ = 250–400 nm, intensity of ~100 W cm^{-2}, Fusion Cure System, Minuta Tech, Korea) for ~30 s, the PET film with the each polymeric HAR nanopillar structure was gently separated from the Si master. During UV exposure, the initiators generate free radicals that react with the acrylate groups of the PUA prepolymer, leading to free radical polymerization and the formation of the crosslinked polymer network (Fig. S1, ESI†).[23] Similarly, the polydimethylsiloxane (PDMS, Sigma Aldrich, Korea) mixture with a mass ratio of precursor: curing agent = 10 : 1 was cast on the Si master and peeled off after thermal curing for an 1 h in an oven at 70 °C.

Recovery of the clustered PUA nanopillars

PUA 301 was dispensed on the clustered nanopillars and covered with a PET film. After the same UV curing process described above, the PET film was gently peeled off from the substrate. During the process, an external force (>3.7 N cm^{-2}) was applied on the clustered nanopillars, resulting in recovering of the pillars.

Characterization

The transmittance of the pristine and clustered nanopillars on PET films was measured on a UV-VIS spectrometer (PerkinElmer Lambda 45, USA) from 300 to 800 nm. PET was used as a reference. The morphologies of the nanopillars under various conditions were imaged using a field emission scanning electron microscope (FE-SEM, AURIGA, Carl Zeiss, Germany) at 5 kV. To measure the contact angles (CAs) of water droplets, we used a contact angle analyser (DSA100, Kruss GmbH., Germany).

Results and discussion

The HAR nanopillar arrays (400 nm in diameter, D, 1 μm in spacing, S, and 4 μm in height, H, see Fig. 1a) are fabricated by molding from a silicon master (see Fig. S2, ESI†) with the corresponding array of nanoholes. The aspect ratio (AR = H/D) of the nanopillars is 10. After filling UV-curable polyurethane acrylate (PUA, MINS 301), which we refer here as PUA 301, into the nanohole array, followed by UV curing, we peel off the polymeric nanopillars from the silicon master. PUA is an elastomeric, versatile molding material that has been used in various soft lithography applications, including bioinspired micro/nanostructures,[22,24] microfluidic devices, and tissue engineering,[25–27] due to its unique properties such as moldability, high strength, and optical transparency.

To fabricate stable HAR nanopillars without failure such as ground collapse (*i.e.*, pillars falling on the ground) or lateral collapse (*i.e.*, pillar clustering), it is important to choose materials with a high elastic modulus and low surface tension.[28] Roca-Cusachs *et al.* have derived the critical modulus of ground collapse as,[28,29]

$$E_c^G = \frac{103(1-\nu^2)^{0.25} H^{1.5} W}{(\pi D)^{2.5}} \quad (1)$$

where ν is the Poisson's ratio and W is the work of adhesion. For PUA 301, ν = 0.3 and W = 38.6 mJ m^{-2},[30] we calculate E_c^G as 17.5 MPa.

For lateral collapse, the critical modulus is ref. 28, 31 and 32

$$E_c^L = \frac{0.94(1-\nu^2)^{0.25} H^3 W}{D^{2.5} S^{1.5}} \quad (2)$$

where S is the spacing distance between pillars. E_c^L = 22.4 MPa. It is noted both eqn (1) and (2) are derived for cylindrical pillars. PUA 301 has E = 19.8 MPa,[33] which indicates that the PUA301 nanopillars are stable for ground collapse but unstable for lateral collapse when external forces are applied to the pillars. We find that the PUA nanopillars do not collapse after peeling off from the silicon master (Fig. 1 and Fig. S3, ESI†), which is due to the fact that the C_4F_8 deposited on the Si master is very efficient in releasing PUA 301, which is relatively hydrophilic (more details in the Experimental section). In comparison, it is difficult to obtain stable nanopillars from PDMS, which are ground collapsed (Fig. S3, ESI†) after peeling off the

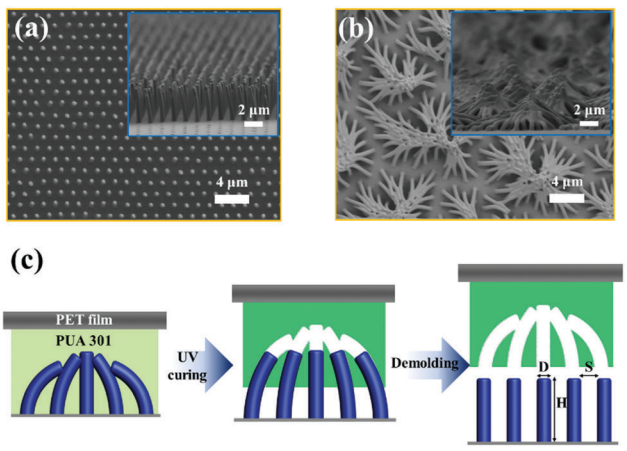

Fig. 1 Top-view SEM images of the straight (a) and clustered (b) HAR nanopillar arrays. Insets: Cross-sectional SEM images of the pristine and clustered HAR nanopillar arrays. (c) A schematic illustration of the shape recovery process of PUA nanopillars by mechanical pulling during demolding.

Si master due to its low elastic modulus (γ = 21.3 mJ m^{-2}, $E \sim 2$ MPa).[28] Straight nanopillars can be obtained from the higher modulus materials, including hard PUA (MINS 311, referred to as PUA 311, E = 350–10 000 MPa)[33] and a conventional UV curable adhesive (NOA 71, γ = 40 mJ m^{-2}, E = 380 MPa).[34] However, most of them are found to be stuck in the Si master which has HAR nanoholes (Fig. S3, ESI†), possibly due to the weak elongation tensile strength (break point of MINS 311 = 9% of elongation and MINS 301 = 45% of elongation)[35] and high adhesion force between NOA 71 and the master. We note that the pillars studied here are cylindrical. Previously, we successfully fabricated tapered nanopillars with high-aspect-ratios (up to 10) from PUA 311.[33] The tapered pillars have a smaller diameter at the tip than the base, and thus a larger interpillar spacing at the top. As a result, the bending moment drastically decreases, and the tapered nanopillars are highly stable without clustering. In contrast, cylindrical nanopillars (aspect ratio ~3) made from even stiffer epoxy (E = 3 GPa) collapsed, but the tapered nanopillars of the same base diameter remained stable.[36]

Typically, once the dense and elastic HAR nanopillars are clustered (Fig. 1b) it is difficult to recover them due to large van der Waals interactions between the clustered pillars. Recently, tilted and low aspect ratio (AR $\leq$ 3) micropillars (diameter, 10 μm) made of shape memory polymers (SMPs) have been demonstrated to recover to their original shapes.[20,37] It is critical that the elastic recovery energy is large enough to overcome the adhesion energy between pillars. Since the elastic strain energy is proportional to the dimension of the pillars as D^3, while the surface energy is proportional to D^2,[37] a decrease of the pillar diameter from 10 μm to 400 nm (in our experiments) dramatically increases the contribution of the surface energy by 625 times. Therefore, the surface energy becomes dominant in HAR nanopillars. Once clustered, nanopillars cannot be recovered without application of an external force. Here, we demonstrate a simple yet versatile approach using mechanical pulling during a demolding process, allowing for repeatable usage of the polymeric HAR nanopillar arrays even after they are clustered. As seen in Fig. 1c, first, the liquid prepolymer of PUA 301 is placed on top of the clustered pillars, followed by capillary infiltration into the space between the pillars. After UV curing, the pillars are mechanically pulled against the crosslinked PUA 301. Here, a deflection force of bent pillars is applied opposite to the adhesion force between pillars (see Fig. 2). The adhesion force between pillars is described as,[26,33]

$$F_{\mathrm{adh}} = \frac{AR^{1/2}l}{16D_{\mathrm{c}}^{2.5}} \quad (3)$$

where A is the Hamaker constant (2.09×10^{-20} J), R is the radius of the pillars (200 nm), l represent the overlap length, ~10% of the pillar height (4 μm), and D_{c} is a cutoff length of the adjacent clustered pillars (0.4 nm). The deflection force is expressed as[26,33]

$$F_{\mathrm{def}} = \frac{3EI\delta}{H^3} \quad (4)$$

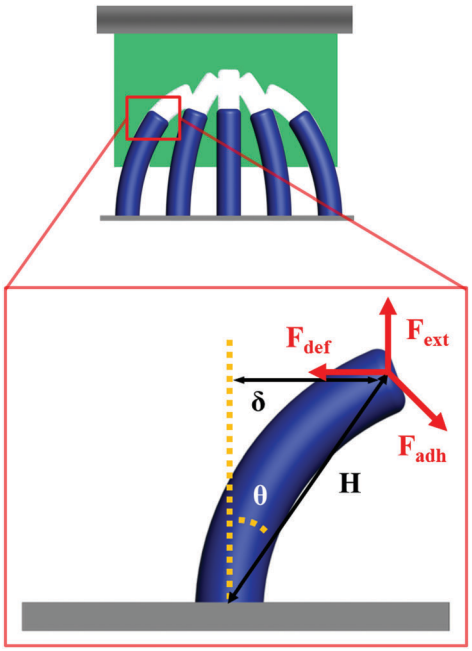

Fig. 2 Schematic illustration of the adhesion force, deflection force, and external force applied to the pillars.

where $I\left(=\frac{\pi R^4}{4}\right)$ is the moment of inertia of the pillars, δ is the deflection of the fabricated original pillars, and H is the height of the pillars (4 μm). When the adhesion force between the clustered pillars is larger than the deflection force, it is not possible to recover the clustered pillars. In our materials system, the calculated adhesion force is $F_{\mathrm{adh}} \sim 3.7$ N cm^{-2} and the deflection force is 0.24 N cm^{-2} considering the largest value of $\delta \sim H$. Therefore, the external pull-off force has to overcome the adhesion force in order to recover the original shape of the nanopillars.

As mentioned, the as-fabricated PUA nanopillar arrays could be collapsed or deformed by an external force during sample handling, mechanical pressing or drying (Fig. 1a and 3b). Here, to induce clustering, we dip the straight PUA HAR nanopillars in a water bath for 3 min, followed by drying in an oven at 40 °C for more than 1 h. Subsequently, we attempt the recovery of the clustered nanopillars by the demolding process with an external pull-off force (F_{ext}) measured as ~10.8 ± 1.1 N cm^{-2} (see Fig. S4, ESI†), which is larger than the adhesion force per area, $F_{\mathrm{adh}} \sim 3.7$ N cm^{-2}, between the clustered pillars as shown in Fig. 1c and 3c. It is important to note that the morphology of the recovered PUA structures is almost identical to their original shapes over a large area (~10 cm × 7 cm, see Fig. S2, ESI† and Fig. 3c). We also note that the elastomeric nature of PUA plays a critical role here. If the pillars are too soft, during demolding, they could ground collapse instantaneously as seen in the case of the PDMS pillars. If the pillars are too stiff and adhesive, they will be stuck into the mold or become fractured during demolding as seen in the case of PUA 311 and NOA 71 nanopillars.

We repeat the clustering/recovery process over 20 cycles. As seen in Fig. 4a, after 5 cycles, there is no deterioration of the

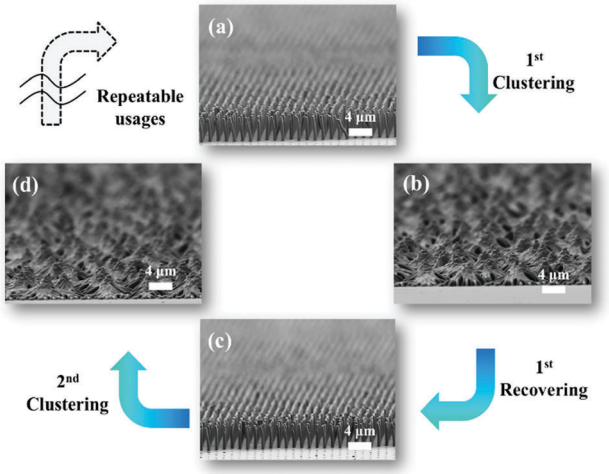

Fig. 3 SEM images of the original (a)/recovered (c) and clustered (b and d) PUA nanopillar arrays.

pillars. After 20 cycles, nanopillars in some regions are detached from the substrate, possibly due to the degradation of the mechanical properties of nanopillars during repeated UV exposure. Nevertheless, the majority of the nanopillars remained intact and returned to the original shape after 20 cycles. Also, we demonstrate controllable wetting with the recovery process. Water contact angles (CAs) are measured on clustered and recovered nanopillars over 20 cycles. As a result of the pillar deformation and recovery, their wettability and optical properties are also changed. As shown in Fig. 4(b), the water contact angle (CA) is $\sim 65^\circ$ on the clustered nanopillars and recovers to $\sim 120^\circ$ after the demolding process. A slight decrease of CAs is observed after 20 cycles of the clustering/recovery processes, which is reasonable given the fact that some nanopillars are degraded as seen in Fig. 4a.

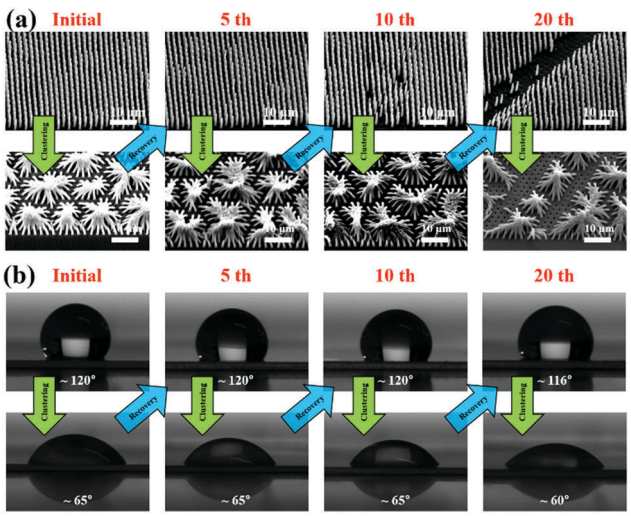

Fig. 4 (a) SEM images of the clustered/recovered PUA nanopillar arrays during 20 cycles of the clustering/recovery process. (b) Optical microscopic images of water contact angles (CAs) measured on the clustered/recovered PUA nanopillar surfaces.

Moreover, the region with clustered HAR nanopillars becomes opaque (Fig. 5a) due to random light scattering, in agreement with our earlier observation.[9] In the case of the straight and recovered nanopillars, they are highly ordered and perpendicular to the air/film interface; they can reflect the light and appear colored when viewed from a low incident angle. Because PUA itself is quite transparent, the transmittance is high when viewed in the normal direction. As seen in Fig. 5b, the average transmittance of the recovered nanopillar film in the normal direction is $\sim 89\%$, similar to that of the reference (PET) in the wavelength range from 300 to 800 nm, whereas the transmittance of the clustered nanopillar film decreases to $\sim 75\%$. After the shape recovery of the nanopillars by the mechanical pulling process, transmittance returns back to $\sim 89\%$.

Lastly, we exploit the local recovery in the selective region using a rigid patterned stamp made of wood block (see Fig. 6a). At first, the film consisting of straight nanopillars is reflective (Fig. 6b). Here, the nanopillar film is placed on a black background to enhance the contrast, thus, the reflective color is more obvious compared to that seen on a PET film in Fig. 5. When applying a force by pressing the patterned stamp against the straight pillars, the pressed region becomes blurred because

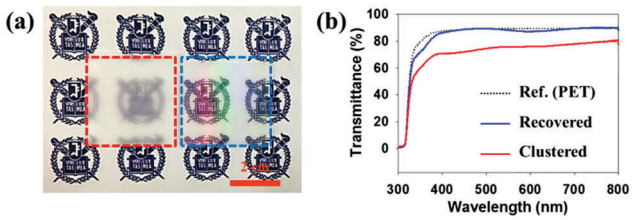

Fig. 5 (a) An optical image of two PUA nanopillar films placed on top of the Seoul National University logo. The opaque film on the left has clustered pillars. The transparent one on the right with reflective colors has straight nanopillars. (b) Transmittance spectra of three different samples: reference (bare PET film), clustered and recovered nanopillar arrays.

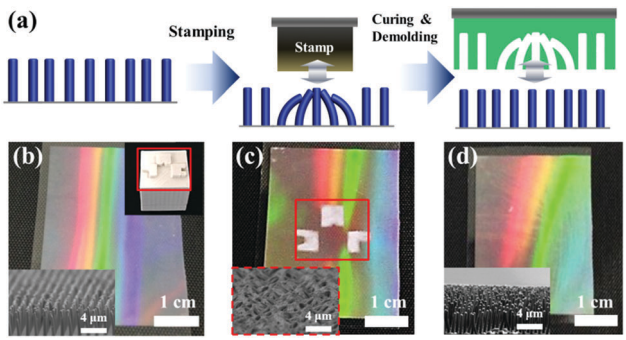

Fig. 6 (a) Schematic illustration of the nanopillar clustering process by stamping a patterned seal and the subsequent shape recovering process *via* demolding. (b–d) Photographs of the PET films with HAR nanopillar arrays. (b) The as-fabricated nanopillars. (c) The stamped region becomes opaque indicating that the pillars are clustered together. (d) Pillars recovered in the stamped regions, thus, recovering the color in the film. The inset in (b) shows the patterned seal. The inset SEM images in (b–d) show the shape of nanopillars in the stamped region.

of the clustering of the nanopillars, displaying the pattern from the stamp (Fig. 6c). After infiltrating the nanopillars with the PUA precursor, followed by curing and pulling, the stamped pattern is erased and the film regains its original reflective color (Fig. 6d), indicating the complete recovery of the pillars.

Conclusions

We investigate the reversible shape recovery of clustered HAR nanopillars through the mechanical pulling during the demolding process of UV curable PUA over a large area. Shape recovery is possible due to the elastic recovery of the clustered nanopillars assisted with the external pull-off force, overcoming the adhesion force between the nanopillars. By taking advantage of the reversible recovery of the clustered nanopillars, we demonstrate stamping and erasing of patterns due to the difference in the optical properties in the clustered region *vs.* the pristine (or recovered) region. With the ability to reversibly and spatially control the clustering and recovery of the nanopillars using mechanical pulling, our method is highly versatile to create smart surfaces.

Acknowledgements

This work was supported by the Global Frontier R&D Program on Center for Multiscale Energy System funded by the National Research Foundation of Korea under the Ministry of Science, ICT & Future Planning, Korea (NRF-2011-0031561), the Basic Science Research Program (2013R1A2A2A04015981), the Commercialization Promotion Agency for R&D Outcomes Grant funded by the Korean Government (MSIP) (2015, Joint Research Corporations Support Program), the R&D Convergence Program of NST (National Research Council of Science & Technology) of Republic of Korea and the Development of Advanced 3D Printing Technology for the Realistic Artificial Hand funded by KIST-ETRI projects. SY acknowledges partial support from National Science Foundation (NSF), grant #CBET-1264808.

References

1 A. K. Geim, S. Dubonos, I. Grigorieva, K. Novoselov, A. Zhukov and S. Y. Shapoval, *Nat. Mater.*, 2003, **2**, 461–463.
2 M. Micciché, E. Arzt and E. Kroner, *ACS Appl. Mater. Interfaces*, 2014, **6**, 7076–7083.
3 W. K. Cho and I. S. Choi, *Adv. Funct. Mater.*, 2008, **18**, 1089–1096.
4 S.-S. Yoon and D.-Y. Khang, *ACS Appl. Mater. Interfaces*, 2013, **5**, 13441–13447.
5 S. Y. Lee, Y. Rahmawan and S. Yang, *ACS Appl. Mater. Interfaces*, 2015, **7**, 24197–24203.
6 J. Li, H. Yu, S. M. Wong, G. Zhang, X. Sun, P. G.-Q. Lo and D.-L. Kwong, *Appl. Phys. Lett.*, 2009, **95**, 033102.
7 G. Kang, A. Matikainen, P. Stenberg, E. Färm, P. Li, M. Ritala, P. Vahimaa, S. Honkanen and X. Tan, *ACS Appl. Mater. Interfaces*, 2015, **7**, 11452–11459.
8 E. Zanchetta, E. Guidi, G. Della Giustina, M. Sorgato, M. Krampera, G. Bassi, R. Di Liddo, G. Lucchetta, M. T. Conconi and G. Brusatin, *ACS Appl. Mater. Interfaces*, 2015, **7**, 7273–7281.
9 D. Chandra and S. Yang, *Langmuir*, 2009, **25**, 10430–10434.
10 H. E. Jeong, S. H. Lee, P. Kim and K. Y. Suh, *Colloids Surf., A*, 2008, **313**, 359–364.
11 S. H. Kang, B. Pokroy, L. Mahadevan and J. Aizenberg, *ACS Nano*, 2010, **4**, 6323–6331.
12 H. G. Duan, J. K. W. Yang and K. K. Berggren, *Small*, 2011, **7**, 2661–2668.
13 J. J. Hill, K. Haller, B. Gelfand and K. J. Ziegler, *ACS Appl. Mater. Interfaces*, 2010, **2**, 1992–1998.
14 M. Matsunaga, M. Aizenberg and J. Aizenberg, *J. Am. Chem. Soc.*, 2011, **133**, 5545–5553.
15 M. De Volder and A. J. Hart, *Angew. Chem., Int. Ed.*, 2013, **52**, 2412–2425.
16 S. H. Kang, N. Wu, A. Grinthal and J. Aizenberg, *Phys. Rev. Lett.*, 2011, **107**, 177801.
17 B. Pokroy, S. H. Kang, L. Mahadevan and J. Aizenberg, *Science*, 2009, **323**, 237–240.
18 D. Wu, Q. D. Chen, B. B. Xu, J. Jiao, Y. Xu, H. Xia and H. B. Sun, *Appl. Phys. Lett.*, 2009, **95**, 091902.
19 Y. Zheng, J. Li, E. Lee and S. Yang, *RSC Adv.*, 2015, **5**, 30495–30499.
20 C. M. Chen and S. Yang, *Adv. Mater.*, 2014, **26**, 1283–1288.
21 H. Liu, B. Lei, W. Jiang, Y. Li, L. Yin, B. Chen and Y. Shi, *RSC Adv.*, 2016, **6**, 16640–16644.
22 S. M. Kang, S. M. Kim, H. N. Kim, M. K. Kwak, D. H. Tahk and K. Y. Suh, *Soft Matter*, 2012, **8**, 8563–8568.
23 S. M. Kang and H. Yoon, *RSC Adv.*, 2016, **6**, 41313–41316.
24 W. G. Bae, H. N. Kim, D. Kim, S. H. Park, H. E. Jeong and K. Y. Suh, *Adv. Mater.*, 2014, **26**, 675–699.
25 K. J. Jang and K. Y. Suh, *Lab Chip*, 2010, **10**, 36–42.
26 M. K. Kwak, H. E. Jeong, T. I. Kim, H. Yoon and K. Y. Suh, *Soft Matter*, 2010, **6**, 1849–1857.
27 M. S. Kim, A. Y. Kim, K. J. Jang, J. H. Kim, J. B. Kim and K. Y. Suh, *Nanotechnology*, 2011, **22**, 494017.
28 Y. Zhang, C.-W. Lo, J. A. Taylor and S. Yang, *Langmuir*, 2006, **22**, 8595–8601.
29 P. Roca-Cusachs, F. Rico, E. Martinez, J. Toset, R. Farré and D. Navajas, *Langmuir*, 2005, **21**, 5542–5548.
30 C. Lee, S. M. Kim, Y. J. Kim, Y. W. Choi, K.-Y. Suh, C. Pang and M. Choi, *ACS Appl. Mater. Interfaces*, 2015, **7**, 2561–2568.
31 N. Glassmaker, A. Jagota, C.-Y. Hui and J. Kim, *J. R. Soc., Interface*, 2004, **1**, 23–33.
32 C. Hui, A. Jagota, Y. Lin and E. Kramer, *Langmuir*, 2002, **18**, 1394–1407.
33 C. Pang, T. I. Kim, W. G. Bae, D. Kang, S. M. Kim and K. Y. Suh, *Adv. Mater.*, 2012, **24**, 475–479.
34 P. Kim, H. Y. Kim, J. K. Kim, G. Reiter and K. Y. Suh, *Lab Chip*, 2009, **9**, 3255–3260.
35 S.-J. Choi, H. N. Kim, W. G. Bae and K.-Y. Suh, *J. Mater. Chem.*, 2011, **21**, 14325–14335.
36 Y. Cho, G. Kim, Y. Cho, S. Y. Lee, H. Minsky, K. T. Turner, D. S. Gianola and S. Yang, *Adv. Mater.*, 2015, **27**, 7788–7793.
37 J. Li, J. Shim, J. Deng, J. T. Overvelde, X. Zhu, K. Bertoldi and S. Yang, *Soft Matter*, 2012, **8**, 10322–10328.

